

# Small Uncrewed Aircraft Based Microphysical Measurements of Polar Stratus Cloud During The Pallas Cloud Experiment 2022

Jessica Girdwood<sup>1,2</sup>, David Brus<sup>3</sup>, Konstantinos-Matthaios Doulergis<sup>3</sup>, and Alexander Böhmländer<sup>4</sup>

<sup>1</sup>Department of Earth, Atmospheric and Environmental Sciences, University of Manchester, Manchester, M13 9PL, UK

<sup>2</sup>National Centre for Atmospheric Science, Department of Earth, Atmospheric and Environmental Sciences, University of Manchester, Manchester, M13 9PL, UK

<sup>3</sup>Finnish Meteorological Institute, Atmospheric Composition Research - Aerosols and Climate, Erik Palménin aukio 1, FI-00560, Helsinki, Finland

<sup>4</sup>Institute of Meteorology and Climate Research, Atmospheric Aerosol Research (IMK-AAF), Karlsruhe Institute of Technology (KIT), Karlsruhe, 76121, Germany

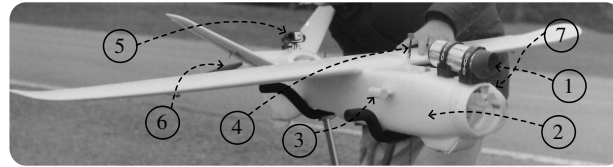
**Correspondence:** Jessica Girdwood (jessica.girdwood@ncas.ac.uk)

**Abstract.** A dataset of in-situ observations of stratus cloud microphysics was created from measurements performed at the Pallas atmosphere-ecosystem super site. The data were collected using a small uncrewed aircraft (SUA) and the low-cost, lightweight Universal Cloud and Aerosol Sounding System (UCASS, Smith et al., 2019). Data from the instrument – platform combination was previously validated in Girdwood et al. (2022b) during a similar field campaign at the same site. The dataset contains cloud droplet size distribution, number concentration, and mass concentration, in addition to geolocation data, and meteorological variables. The flight pattern of the SUA was planned to provide a quasi-vertical profile. A total of 84 of these profiles across 39 flights were performed during the campaign period. The data from the SUA flights are available from 10.5281/zenodo.14756233 (Girdwood et al., 2022a).

## 1 Introduction

Clouds are inadequately represented in models of climate change, and thus contribute to large uncertainties in effective radiative forcing (Maschelinotte et al., 2021). In addition, many cloud processes are not sufficiently well understood or characterised to adequately represent in weather models, leading to errors in forecasting precipitation and fog. In-situ cloud microphysical measurements are essential for targeted studies of cloud processes, validation of remote sensing retrievals, and development thereof. One of the reasons for this is a lack of effective measurement, due to the limited capability of conventional platforms; conventional aircraft cannot fly through a cloud with a high enough spatial resolution, due to manoeuvrability limitations. In addition, cloud in-situ instrumentation is often deployed in a prototype stage, and requires significant calibration, characterisation, and validation for appropriate data utilisation in models and cloud research.

Small uncrewed aircraft (SUA) as a measurement platform have the potential to part-fill the measurement gap in in-situ cloud microphysics. This is because they are often small and manoeuvrable, meaning they can be piloted through a cloud with high spatial resolution when compared to conventional aircraft. In addition, SUA often carry lower financial risk when compared



- |                       |                            |
|-----------------------|----------------------------|
| 1. UCASS Probe        | 5. Video Camera            |
| 2. FMI-Talon SUA      | 6. Rearward Propeller      |
| 3. Met Sensor Package | 7. Pitot Tube (Other Side) |
| 4. Telemetry Antennae |                            |

**Figure 1.** A picture of the FMI-Talon SUA in the configuration which was used for the campaign. The various components of the instrument platform are marked.

with conventional aircraft, which increases the accessibility of cloud physics to researchers without access to conventional aircraft.

However, calibration and validation of instrumentation is particularly important when considering SUA cloud in-situ instrumentation, since such instruments are usually lightweight and low cost. Platform-instrument synergy is of paramount importance when considering SUA measurements due to the wide array of platforms, and the complex aerodynamics surrounding airframes. Recent efforts have been made to validate the Universal Cloud and Aerosol Sounding System (UCASS, Smith et al., 2019) with the Talon SUA from the Finnish Meteorological institute (FMI-Talon). Girdwood et al. (2022b) conducted experiments to compare cloud in-situ measurements from the FMI-Talon – UCASS combination with a reference instrument mounted on a hilltop, in addition to computation fluid dynamics with Lagrangian particle tracking (CFD-LPT) to influence the design of the system. The UCASS is an optical particle spectrometer (OPS), which measures the scattering cross section of cloud particles. This can be translated into a physical radius via the means of a scattering model based retrieval.

In this paper, we use the system presented in Girdwood et al. (2022b) to measure the microphysics of arctic warm stratus cloud. We implement automated data quality assurance (QA), and add derived products such as number concentration and effective diameter to the dataset, which is available from Girdwood et al. (2022a).

## 35 2 Methods


### 2.1 Apparatus

The UCASS was attached to the FMI-Talon using the same mounting points as described in Girdwood et al. (2022b). This was in order to ensure that the characterisation of the platform was still valid in this situation. Positional data pertaining to the SUA were obtained from a Global Navigation Satellite System (GNSS), which was also used for flight automation. An inertial measurement unit (IMU) was also included in the flight controller of the SUA, which was used to obtain the airframe orientation data necessary for quality assurance. A pitot tube (noa, a) was used to obtain airspeed data, which were necessary to

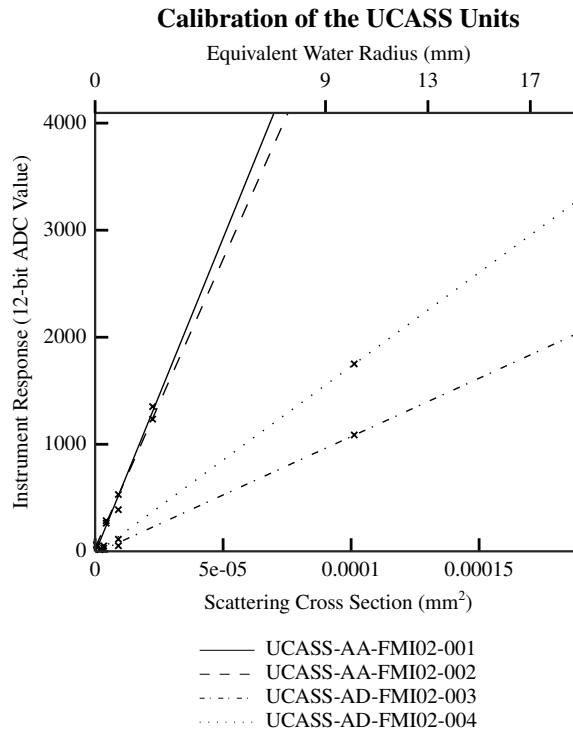


**Figure 2.** A graph showing the different calibration curves of the UCASS units which were used for the campaign. The serial numbers for the four instruments are stated in the key. The calibration data points were marked on the graph with an 'x'.

calculate particle concentrations from the UCASS, in addition to data quality assurance. An annotated image of the FMI-Talon is shown in Fig. 1.

The detailed schematics and working principles of the UCASS can be found in Smith et al. (2019) and Girdwood (2023), however this can be briefly summarised as: 650 nm light was scattered off of a cloud droplet, which was then collected by an ellipsoidal mirror and reflected onto a photodiode, whereupon the magnitude of the scattered light is measured and recorded. The UCASS units used in this paper were calibrated using the aerosol calibration method described in Girdwood et al. (2025). There were two possible transimpedance amplifier gain modes in which the units could be set: low gain and high gain, which had size ranges of approximately 3 to 40  $\mu\text{m}$  and 0.4 to 15  $\mu\text{m}$  respectively. The exact size ranges depended on the instrument calibration coefficients. A total of four UCASS units – two low gain and two high gain variants – were deployed throughout this campaign, the calibrations for which are shown in Fig. 2. The UCASS unit which was used at any one time was chosen based on availability, and the presence of clouds – a low gain unit was used for measurements of cloud droplets and a high gain unit was used for measurements of aerosol. 

Thermodynamic measurements of temperature and humidity were obtained from an SHT85 (AG) sensor which was positioned in a radiation shielding housing. However, this sensor was rendered inoperable part way through the campaign due to an issue

with moisture ingress, and was therefore replaced with a BME280 (noa, b). The data were logged from three separate sources: the flight data and housekeeping, including GNSS and IMU data, were logged on the SUA flight controller; meteorological data were logged on a Raspberry Pi Zero (Ltd) with a frequency of 1 Hz; and the UCASS data were logged on a separate Raspberry Pi Zero with a sample frequency of 2 Hz.



## 60 2.2 Flight Information and Constraints

During the month long intensive part of the field campaign, a total of 39 SUA flights were conducted. A flight consisted of a profile – or series thereof – up to the maximum allowed ceiling of 2 km above ground level. A total of 84 profiles were extracted from the data, see Sect. 3.3 for more information. The SUA flight controller firmware was capable of facilitating waypoint navigation, meaning that a series of GNSS waypoints could be programmed before a flight, then the SUA would follow this flight plan. The waypoints were positioned in a vertical ‘zig-zag’ switchback pattern with the aim of creating a quasi-vertical profile which was constrained to a lateral deviation of no more than 1 km, however wind conditions often necessitated operating beyond this. The switchback pattern was programmed to be laterally parallel with the wind direction to minimise deviations from the  $15^\circ$  of attack (AoA) limit defined in Girdwood et al. (2022b). The airspeed acceptance limit of the UCASS, as determined by the bandwidth of the amplification and signal conditioning electronics, was  $20 \text{ ms}^{-1}$ . Therefore, the desired cruising speed was adjusted accordingly to  $15 \text{ ms}^{-1}$ . Since there were times that the SUA had to stray beyond the AoA and airspeed limits for manoeuvres and operational necessity, it was determined that the most pragmatic approach would be to apply these limits as a data quality assurance (QA) step.

The flights took place at the Pallas atmosphere-ecosystem super site. This is located 170 km north of the Arctic Circle ( $67.973^\circ\text{N}$ ,  $24.116^\circ\text{E}$ ), partly in the area of Pallas-Yllästunturi National Park (Lohila, Annalea et al.). A map of the SUA operation area, in addition to an example flight, is shown in Fig. 3.

## 3 Data

### 3.1 Software

The data were processed using the "oproc" python package, which was custom made for integrating OPS data with meteorological and geolocation data, and can be found on GitHub (Girdwood, 2025). This package is capable of processing raw data from an indeterminate number of files and synchronising it to a global time step which, in this instance, was set to 0.5 s. This was necessary because the meteorological data, the UCASS data, and the flight controller data were all recorded on different data loggers at different time steps.

The software uses a configuration file which allows the user to specify which raw files are desired, which columns and rows are needed from each file, and the units of all the variables. Unit conversion is handled automatically by referencing the specified variables against a central database, which can be altered by the user if desired. While the package was created with the intention of analysing OPS data specifically, it can also be used as a processing framework for general meteorological data.

### First Profile of Flight 001

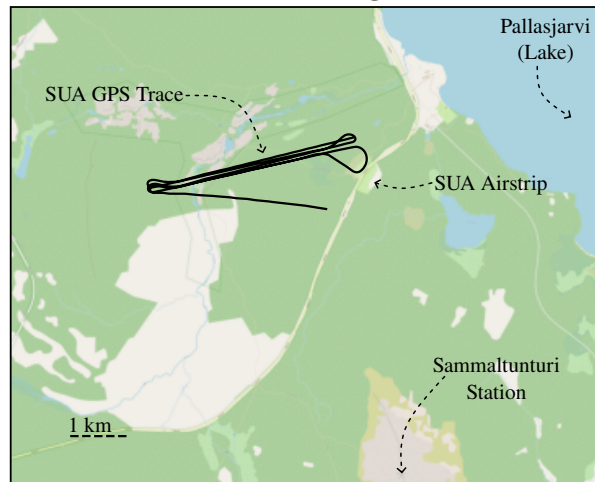


**Figure 3.** A map of the SUA operations area which was active for the campaign period. The latitude-longitude trace for flight ‘001’ – see Table 2 for more information – is also shown on the map as an example. The data for the map were obtained from OpenStreetMap contributors (2017) © OpenStreetMap contributors 2025. Distributed under the Open Data Commons Open Database License (ODbL) v1.0.

Once the data are imported, they can be processed using **one of a number of algorithms**, which are referred to in the software as "proc" objects, because they are subclasses of a class called "\_\_Proc". This is to ensure that the processing of units is consistent, and that all the required variables are present. Once the data are imported they can be saved in an HDF5 file in which the units and descriptions of each variable are also stored as metadata.

All processing, data extraction, and plotting can be done in this software, which additionally includes space for customisation and addition of user specified processing routines.


### 3.2 Data Analysis and QA

95 Since the constraining conditions the UCASS were occasionally breached due to operational necessity, data QA was needed. In order to do this a series of data QA variables, which will henceforth be referred to as "masks", were created. A mask variable is a column with the same length as the rest of the data, which has a boolean value. If the mask value resolves as true for a particular row, then this row would be accepted for this mask condition. For example, if one were to create a mask variable for airspeeds above  $20 \text{ ms}^{-1}$ , every row where the airspeed exceeded this limit would be false. The masking variable conditions  
100 for these data were AoA values exceeding  $15^\circ$ , airspeed values exceeding  $20 \text{ ms}^{-1}$ , and profile number. Profile number was calculated based on peaks of time pressure time series, and the mask is true for each row considered to be with profile

**Table 1.** The derived data products which are present in the dataset.

<i>Variable</i>	<i>Unit</i>	<i>Set</i>	<i>Description</i>
Sample Volume	m <sup>3</sup>	Main	The amount of air which the UCASS sample volume passed through. This is derived from airspeed and sample area.
Bin Boundaries	µm	Housekeeping	The bin boundaries of the UCASS. This is provided in terms of scattering cross section and radius of a water droplet. The scattering cross section boundaries require only calibration data, whereas the water droplet radius boundaries require both calibration data and the material lookup table.
Bin Centres	µm	Housekeeping	The bin centres of the UCASS which, similarly to bin boundaries, are provided in terms of both scattering cross section and water droplet diameter. The centre is computed using a geometric mean of the boundaries either side.
AoA	°	Main	The absolute angle between the airspeed vector relative to the UCASS and the position vector of the UCASS.
Corrected Airspeed	ms <sup>-1</sup>	Main	The airspeed of the airframe calculated using ground speed and the wind data from a ground station. This was used when the pitot tube on the SUA was malfunctioning.
Mass Concentration	kgm <sup>-3</sup>	Main	Total mass of the droplets per unit sample volume. This was calculated assuming every particle which was measured by the UCASS was a spherical water droplet. This is equivalent to liquid water content (LWC).
Number Concentration	m <sup>-3</sup>	Main	The number of droplets counted by the UCASS per unit sample volume.
Effective Radius	µm	Main	The ratio of the third to second statistical moments of the droplet size distribution for a particular row.

number. Odd number profiles were ascending in altitude and even number profiles were descending. The AoA for the aircraft was calculated using the procedure described in Girdwood et al. (2022b) and the wind direction from Sammaltunturi station.

105 Occasionally, the pitot tube, which was used to measure airspeed, would get blocked with liquid water or ice while flying through a cloud. This meant that the default airspeed would be unusable for a profile. In order to compute UCASS data products, a corrected airspeed needed to be derived. This was calculated by using the AoA vector equations from Girdwood et al. (2022b), and obtaining the wind speed and direction from Sammaltunturi n.

Additionally included in the data are some derived data products, which are summarised in Table 1.

### 3.3 Dataset Structure

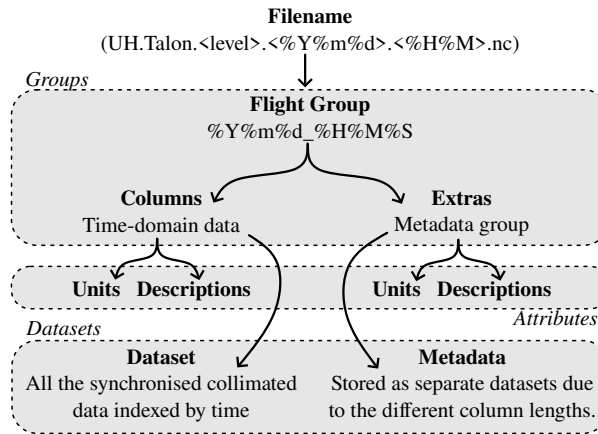


**Figure 4.** An illustration of the structure of the HDF5 files which are in the dataset. The groups, attributes, and dataset file structures are labelled.

A summary of the contents and processing of all the data files provided is shown in Table 2. The data in the set came from three different data loggers – one for UCASS, one for the flight controller, and one for the meteorological data – which occasionally malfunctioned or were unavailable due to repair. The data sources which were available for each file are shown in Table 2. The meteorological data logger is split into "SHT" and "BME" because, for the first part of the campaign, a Senserion SHT85 sensor was used (AG), and for the latter part of the campaign a Bosh BME280 (noa, b) was used.

The data level is also included here. If the flight controller data were not available for a particular flight, then no further processing could be conducted since both airspeed and corrected airspeed require flight controller data, and these are used to compute all the derived data products. In addition, flight controller data, specifically attitude and position data, are used to perform the automated QA process. These flight files are therefore left at level "a1", while the rest are processed to level "c1". Examples of the level "c1" data are presented in Fig. 5 and Fig. 6, where plots of number concentration and effective radius versus altitude for the intensive campaign period are shown. The flight number is shown on both of these plots, and for brevity only the first profile (the first upwards leg) is shown in each one.

Also included in Table 2 is the number of profiles which were performed in each flight, which varied depending on weather conditions, battery capacity, and other operational constraints. The total number of profiles performed over the campaign period was 84, which includes downwards profiles, and excludes all flights where flight controller data were unavailable, since the total number of profiles cannot be known in this case.

Each flight is in one single file named following the constraints outlined in Brus, D. et al. (2025). The file format is HDF5; within each file is a master group with the flight date and time in format ‘%Y%m%d\_%H%M%S’. Within this master group are two subgroups called ‘columns’ and ‘extras’, which contain the synchronised collimated data and the housekeeping data

**Table 2.** A summary of all the flights, to which level they are processed, and which data sources are in each file. Also included here is the airspeed type used for processing and the number of profiles



<i>Flight Number</i>	<i>Date</i>	<i>Time</i>	<i>Data Level</i>	<i>SHT</i>	<i>BME</i>	<i>UCASS</i>	<i>Flight Controller</i>	<i>Airspeed Type</i>	<i>Number of Profiles</i>
01	2022-09-20	14:10	c1	.	.	.	.	Normal	4
02	2022-09-21	09:09	c1	.	.	.	.	Normal	4
03	2022-09-21	14:49	c1	.	.	.	.	Normal	4
04	2022-09-22	09:20	c1	.	.	.	.	Normal	4
05	2022-09-22	10:14	a1	.	.	.	.	None	n/a
06	2022-09-22	10:39	c1	.	.	.	.	Normal	4
07	2022-09-22	15:06	c1	.	.	.	.	Normal	4
08	2022-09-22	15:55	c1	.	.	.	.	Normal	2
09	2022-09-23	12:13	c1	.	.	.	.	Normal	4
10	2022-09-23	13:05	c1	.	.	.	.	Normal	2
11	2022-09-23	17:33	c1	.	.	.	.	Normal	4
12	2022-09-24	09:42	c1	.	.	.	.	Normal	4
13	2022-09-24	10:38	c1	.	.	.	.	Normal	4
14	2022-09-27	15:21	c1	.	.	.	.	Normal	4
15	2022-09-28	09:21	c1	.	.	.	.	Corrected	2
16	2022-09-28	14:17	c1	.	.	.	.	Corrected	2
17	2022-09-29	12:02	a1	.	.	.	.	None	n/a
18	2022-09-30	10:08	c1	.	.	.	.	Normal	2
19	2022-09-30	11:31	c1	.	.	.	.	Normal	2
20	2022-09-30	17:14	c1	.	.	.	.	Corrected	2
21	2022-10-01	15:11	c1	.	.	.	.	Normal	2
22	2022-10-02	12:33	c1	.	.	.	.	Corrected	2
23	2022-10-02	14:31	c1	.	.	.	.	Corrected	2
24	2022-10-04	10:05	c1	.	.	.	.	Corrected	2
25	2022-10-04	12:19	c1	.	.	.	.	Corrected	2
26	2022-10-04	14:23	c1	.	.	.	.	Corrected	2
27	2022-10-04	15:10	c1	.	.	.	.	Corrected	2
28	2022-10-04	16:32	c1	.	.	.	.	Corrected	2
29	2022-10-05	10:46	a1	.	.	.	.	None	n/a
30	2022-10-07	07:55	c1	.	.	.	.	Normal	2
31	2022-10-07	08:55	c1	.	.	.	.	Normal	4

32	2022-10-07	13:47	c1	.	.	.	Normal	2
33	2022-10-07	14:34	c1	.	.	.	Normal	2
34	2022-10-11	12:46	a1	.	.	.	None	n/a
35	2022-10-11	15:02	a1	.	.	.	None	n/a
36	2022-10-11	15:44	a1	.	.	.	None	n/a
37	2022-10-12	09:55	a1	.	.	.	None	n/a
38	2022-10-12	12:15	a1	.	.	.	None	n/a
39	2022-10-12	15:08	a1	.	.	.	None	n/a

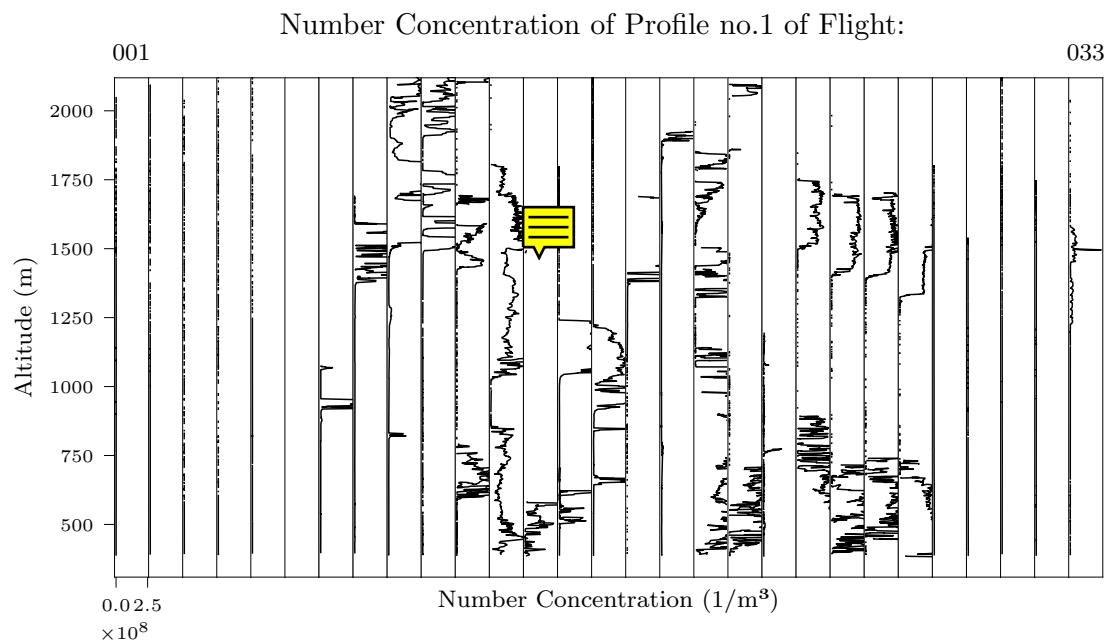


**Figure 5.** The number concentration profiles from the UCASS throughout the intensive campaign period. The flights where flight controller data were not available are omitted from the figure. The flight number, consistent with Table 2, is shown at the top of the graph.

respectively. The units and descriptions of each variable are stored as group attributes, assigned to the ‘columns’ and ‘extras’ groups as appropriate for the specific variable. A graphical depiction of the file structure is shown in Fig. 4.

#### 4 Summary

This manuscript presents the data collected using the UCASS instrument on the FMI-Talon SUA during the intensive period  
 135 of the PaCE 2022 field campaign. This campaign took place during Autumn 2022, with the purpose of investigating polar

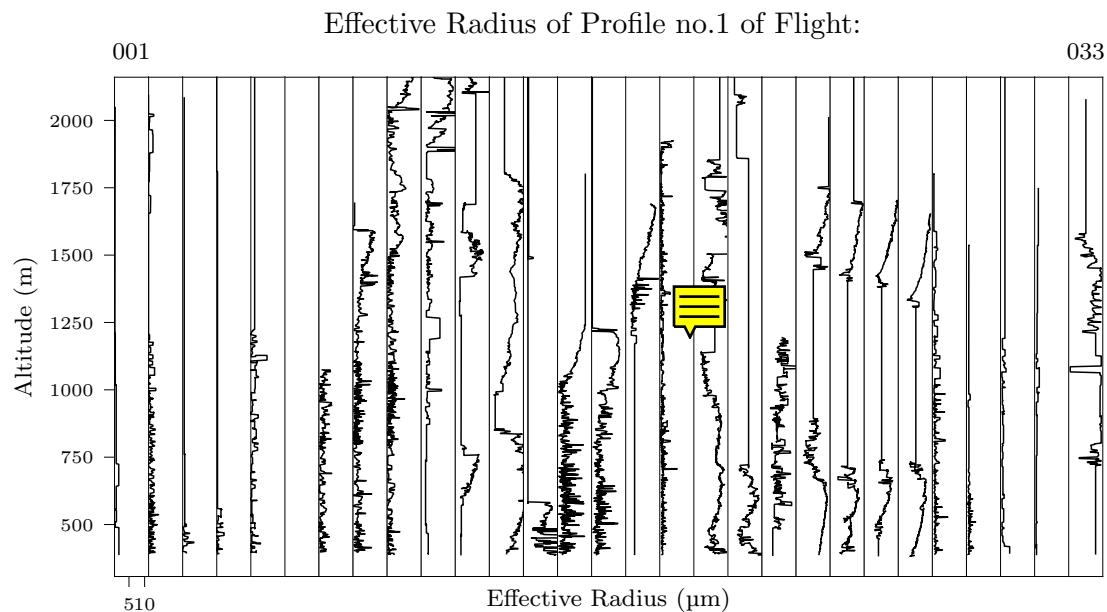


**Figure 6.** Effective radius profiles computed from UCASS data throughout the intensive campaign period. The flight numbers shown on the top of the graph are consistent with Fig. 5.

warm and mixed-phase cloud processes, and the advancement of measurement techniques. The dataset, which can be found in Girdwood et al. (2022a), contains data which was processed to level "c1" – with the exception of flights which did not contain flight controller data which were processed to level "a1" only – using the custom made "oproc" python package, which is available from Girdwood (2025).

140 The methods used for data collection were validated during a separate campaign in Pallas in 2020, the results of which can be found in Girdwood et al. (2022b). The data QA was conducted autonomously using the "oproc" software package. The data from the campaign are published alongside data from other platforms, the overview for which can be found in Brus, D. et al. (2025). It is the intention that these data can be used alongside each-other to provide a more complete picture of the atmosphere for the campaign duration.



145 . **Acknowledgements** Map data copyrighted OpenStreetMap contributors and available from <https://www.openstreetmap.org>. The authors acknowledge the Finnish Meteorological Institute for running the Pallas-Yllästunturi super site, and for providing logistical support throughout the campaign. Some of the fieldwork was funded under the Aerosol, Clouds and Trace Gases Research Infrastructure (ACTRIS) transnational access programme.

. **Code and Data Availability** The dataset is available from 10.5281/zenodo.14756233 (Girdwood et al., 2022a) and the code is available  
150 from Girdwood (2025).

. **Author Contribution** Data were collected by all authors, the manuscript was written by JG and curated by all authors, data curation was conducted by JG, software development was conducted by JG, conceptualisation and supervision was provided by DB.

. **Competing Interests** The authors declare that they have no conflict of interest.

## References

- 155 Digital Air Speed Sensor - MS4525DO, <https://holybro.com/products/digital-air-speed-sensor-ms4525do>, a. Pressure Sensor BMP280, <https://www.bosch-sensortec.com/products/environmental-sensors/pressure-sensors/bmp280/>, b. AG, S.: SHT31-DIS-B -  $\pm 2\%$  (0-100%RH) Digital humidity and temperature sensor, <https://sensirion.com/products/catalog/SHT31-DIS-B>.
- Brus, D., Doulgeris, K., Bagheri, G., Bodenschatz, E., Chávez-Medina, V., Schlenczek, O., Khodamodari, H., Pohorsky, R., Schmale, J., Lonardi, M., Favre, L., Böhmländer, A., Möhler, O., Lacher, L., Girdwood, J., Gratzl, J., Grothe, H., Kaikkonen, V., Molkoselkä, E., Mäkynen, A., O'Connor, E., Leskinen, N., Tukiainen, S., Le, V., Backman, J., Luoma, K., Servomaa, H., and Asmi E.: Data generated during the Pallas Cloud Experiment 2022 campaign: an introduction and overview, *Earth System Science Data*, 2025.
- 160 Girdwood, J.: Optical Measurement of Airborne Particles on Unmanned Aircraft, Ph.D. thesis, University of Hertfordshire, Hatfield, <https://doi.org/10.18745/th.27277>, accepted: 2023-12-11T12:17:55Z, 2023.
- Girdwood, J.: wolkchen-cirrus/UCASSDataProcessor, <https://github.com/wolkchen-cirrus/UCASSDataProcessor>, original-date: 2022-10-01T09:03:27Z, 2025.
- 165 Girdwood, J., Brus, D., and Doulgeris, K.: Data From the Universal Cloud and Aerosol Sounding System Abord an Uncrewed Aircraft During the Pallas Cloud Experiment 2022, <https://doi.org/10.5281/zenodo.14756233>, 2022a.
- Girdwood, J., Stanley, W., Stopford, C., and Brus, D.: Simulation and field campaign evaluation of an optical particle counter on a fixed-wing UAV, *Atmospheric Measurement Techniques*, 15, 2061–2076, <https://doi.org/10.5194/amt-15-2061-2022>, 2022b.
- 170 Girdwood, J., Ballington, H., Stopford, C., Lewis, R., and Hesse, E.: Calibration of optical particle spectrometers using mounted fibres, *Atmospheric Measurement Techniques*, 18, 305–317, <https://doi.org/10.5194/amt-18-305-2025>, publisher: Copernicus GmbH, 2025.
- Lohila, Annalea, Penttilä, Timo, Jortikka, Sinikka, Aalto, Tuula, Anttila, Pia, Asmi, Eija, Aurela, Mika, Hatakka, Juha, Hellén, Heidi, Henttonen, Heikki, Hänninen, Pekka, Kilkki, Juho, Kyllönen, Katriina, Laurila, Tuomas, Lepistö, Ahti, Lihavainen, Heikki, Makkonen, Ulla, Paatero, Jussi, Rask, Martti, Sutinen, Raimo, Tuovinen, Juha-Pekka, Vuorenmaa, Jussi, and Viisanen, Yrjö: Preface to the special issue on integrated research of atmosphere, ecosystems and environment at Pallas, *Boreal Environment Research*, <https://doi.org/http://hdl.handle.net/10138/228278>.
- 175 Ltd, R. P.: Raspberry Pi Zero, <https://www.raspberrypi.com/products/raspberry-pi-zero/>.
- Masson-Delmotte, V., Zhai, P., Pirani, A., Connors, S. L., Péan, C., Berger, S., Caud, N., Goldfarb, L., Gomis, M. I., Chen, Y., Huang, M., Leitzell, K., Lonnoy, E., Matthews, J. R., Maycock, T. K., Waterfield, T., Yelekçi, O., Yu, R., and Zhou, B.: IPCC, 2021: Climate Change 2021: The Physical Science Basis. Contribution of Working Group I to the Sixth Assessment Report of the Intergovernmental Panel on Climate Change, Cambridge University Press, Cambridge, United Kingdom and New York, NY, USA, <https://doi.org/10.1017/9781009157896>, 2021.
- OpenStreetMap contributors: Planet dump retrieved from <https://planet.osm.org> , <https://www.openstreetmap.org>, 2017.
- 185 Smith, H. R., Ulanowski, Z., Kaye, P. H., Hirst, E., Stanley, W., Kaye, R., Wieser, A., Stopford, C., Kezoudi, M., Girdwood, J., Greenaway, R., and Mackenzie, R.: The Universal Cloud and Aerosol Sounding System (UCASS): a low-cost miniature optical particle counter for use in dropsonde or balloon-borne sounding systems, *Atmospheric Measurement Techniques*, 12, 6579–6599, <https://doi.org/10.5194/amt-12-6579-2019>, 2019.